Received: January 3, 2023. Revised: January 25, 2023.

INASS

International Journal of
Intelligent Engineering & Systems

http://www.inass.org/

Development of Predictive Voltage Controller Design for PEM Fuel Cell System based on Identifier Model

Fatima Abdul Sattar AL-Taie[1]* **Ahmed Sabah Al-Araji[1]**

[1]*Computer Engineering Department, University of Technology –Iraq, Baghdad, Iraq*
* Corresponding author's Email: 120121@uotechnology.edu.iq

Abstract: This paper presents a new development of a predictive voltage neural controller to control the stack terminal output voltage of a nonlinear proton exchange membrane fuel cell (PEMFC) system based on a neural network technique and a back-propagation learning algorithm. The main objective of this paper is to precisely and quickly identify the best control action of the hydrogen partial pressure to enhance the nonlinear performance of the fuel cell output voltage under a variable load current. This optimal control action prevents damage to the fuel cell membrane, thereby prolonging the fuel cell's lifetime. The proposed predictive voltage controller consists of three sub-controllers. The first one is the numerical feed-forward controller (NFFC), which is used to decide the steady-state hydrogen partial pressure (PH_2) control action depending on the desired voltage. The second sub-controller is a feedback neural controller that uses a multi-layer perceptron (MLP) and a back-propagation learning algorithm to generate the hydrogen partial pressure feedback control action to track the desired output voltage of the fuel cell during transient conditions. The third sub-controller is the predictive control law equation, which is based on the modified Elman recurrent neural network (MERNN) as an identifier for the PEMFC model and the multi-objective performance index. From the simulation results, the proposed controller, which is composed of the three sub-controllers, has the capability to generate a precisely and quickly timed response to the hydrogen partial pressure control action in order to minimize the tracking voltage error and eliminate oscillation in the output voltage of the fuel cell. Finally, the suggested predictive voltage control strategy's numerical simulation results are then verified by comparison with those of other types of controllers in terms of the minimum number of steps ahead prediction (reducing from 10 to 1 step ahead prediction) and enhancement of the tracking voltage error by 81.8% when comparing with a predictive neural controller and improvement of the tracking voltage error by 87.5% when comparing with an inverse neural controller. Moreover, the oscillation effect in the output voltage is completely eliminated, resulting in a response without any overshoot.

Keywords: Back-propagation algorithm, Modified elman recurrent neural network, Identifier, Predictive controller, PEM fuel cell.

1. Introduction

A significant problem in contemporary life is the worldwide energy shortage. As a consequence of the growing disparity between global energy demands and global energy resources, more focus has been placed on the development of renewable energy sources like solar energy, wind power, and bioenergy, to name a few. In this context, hydrogen fuel cells are attracting global interest that is only going to grow because of their high energy density, low construction costs, and low air pollution [1, 2]. Although this technology was discovered in the 18th century, NASA began utilizing fuel cells in spacecraft carried into orbit in the 1960s and began to market them. The fuel cell's basic operating principle is the production of straightforward electrical energy as a result of a chemical process. To this end, there are many ways to categorize fuel cells, but the electrolyte is the most important one. The most common types are alkaline fuel cells (AFC), phosphoric acid fuel cells (PAFC), molten carbonate fuel cells (MCFC), solid oxide fuel cells (SOFC), and proton exchange membrane fuel cells (PEMFC) [3]. In particular, the PEMFC systems are the most popular hydrogen energy source because they offer the essential qualities of high efficiency,

high reliability, low operating noise, and flexible modular design together with excellent performance, quick power response, high power density, low operating temperature, and low maintenance requirements [4, 5]. As a result, they are widely utilized in military environments, cars, unmanned aerial vehicles, and mobile devices [2]. The PEMFC seems to be an appropriate clean energy generation technology for various applications. To enhance the system's general performance, a few bolts, particularly those connected to its control, still need to be removed. Specifically, improvement in global efficiency, optimum hydrogen and air utilization, and consistent and accurate power response continue to be challenging management objectives [5]. Since fuel cell output voltage and power significantly impact fuel cell performance, researchers have proposed various control strategies to monitor the fuel cell stack's output voltage and power. For instance, the authors in [6] proposed a model reference method utilizing a proportional integral differential (PID) controller. This suggested method maintained a constant voltage despite numerous noises and disturbances. Moreover, to control the PEMFC output voltage, the researchers in [7] swarm optimization based on particle swarm optimization (PSO) is proposed to tune the PID controller parameters in order to improve the dynamic behaviour of the system. Although each of these algorithms has a straightforward structure and is relatively simple to put into practice, due to their weak adaptive capacity, they face extreme difficulty in being adjusted to the nonlinear properties of the PEMFC model. Additionally, these algorithms take a long time to regulate and stabilize, making it practically impossible to attain ideal control performance. Furthermore, the researchers in [8] proposed an NN-based model predictive control (MPC) system. In this system, the rate of hydrogen was controlled by the proposed controller, which was learned by the presented NN to achieve the desired efficiency. For controlling the PEMFC's voltage, [9] presented a model predictive control system, studied the cell's transient behavior, and checked how important it is that input variables affect the voltage of the cell. Likewise, a PEMFC temperature and voltage dynamic management controller using MPC was proposed in [10]. In particular, the mass flow rate of cooling water and hydrogen gas regulate the operating temperature and the output voltage, respectively. Analysis was done on the PEMFC's performance with various controllers, including MPC and conventional PID controllers in terms of response time, output voltage, and temperature overshoots that have markedly decreased. Although such predictive control algorithms can deal with disturbances in complex systems, like the PEMFC, and handle parameter uncertainty within such systems, their substantial reliance on modeling and complicated design makes applying them to practical use quite challenging. In [11], the researchers developed a robust artificial neural feedback controller that can achieve the control on the fuel cell's output voltage through a feed-forward neural network controller with robust optimization method, which is the harmony search method that has a fast response. A max power point tracking (MPPT)- based neural network (NN) and fuzzy logic control (FLC) were utilized in [12] to follow the maximum pick of the output power at various operating temperatures. The outcomes revealed that the suggested neural network MPPT followed the maximum power point more quickly than the FLC. In another work, the duty cycle was used in [13] to regulate the output voltage of FC and track the max power point. In addition, the suggested technique, known as GA-ANFIS, was used to calculate the ideal reference voltages to appropriately regulate the FC output voltage. In [14], the authors proposed an ideal output voltage controller based on distributed deep reinforcement learning and ensemble intelligence exploration multi-delay deep deterministic policy gradient (EIM-DDPG) algorithm, which regulated the PEMFC's fuel input to manage the output voltage. Furthermore, the researcher in [15] proposed a voltage-tracking controller to improve the dynamic behaviour of the output voltage of the PEMFC systems using an inverse neural controller and an HFF-CPSO (hybrid firefly chaotic particulate swarm optimization) algorithm to produce a smooth control action of hydrogen partial pressure and reduced output voltage oscillation. However, the output voltage oscillation was not completely eliminated, and there remains a small error value in the output voltage. A proportional-integral (PI) controller and a sliding mode controller (SMC) were suggested in [16] as a method to keep the fuel cell running at its most productive power level. Although the PI is distinguished by its simplicity, external disturbances and disruptions can negatively affect its performance. The comparison results with the PID controller have shown that the sliding mode controller is distinguished by its stability, particularly against changes in outside influences and disturbances. However, the drawback of this method is that the results were obtained using an offline method without taking into account changes in temperature or changes in the output voltage with the variable current load. In [17], it was suggested to use quasi-continuous high-order sliding mode (QC-HOSM) for PEMFC to

control the output power using a variable current to produce a smooth voltage response, and increase overall system efficiency by reducing oscillation phenomena by achievement the robustness of the conventional SMC. According to the simulation results for the suggested controller in [17], the oscillation influence was reduced, but it was not eliminated.

In this work, the problem definition is that the fuel cell's output voltage varies with step changing the load current and is regarded as a critical problem in the nonlinear fuel cell behavior. As a consequence, a controller that generates the proper value of PH_2 is required in order to supply the necessary voltage during variations in the load current.

Specifically, the goal of this study is to determine the optimal control action value of the hydrogen partial pressure (PH_2) in order to improve the dynamic performance of the nonlinear fuel cell output voltage under variable load current conditions to increase fuel cell longevity and drastically reduce hydrogen consumption by implementing the proposed online predictive neural controller.
This paper's primary contribution is to:

- Research and evaluation how the output voltage of the nonlinear model of the PEMFC responds to variations in the input value of the hydrogen partial pressure, the output current of the fuel cell, and temperature.
- Construct a neural network identifier for the nonlinear PEMFC model using the recurrent neural networks (modified Elman recurrent neural network) to overcome the difficulty of the mathematical model of the fuel cell in terms of finding the Jacobian function and attaining quick learning without oscillation in the output identifier model.
- Develop a numerical inverse feed-forward controller to rapidly and precisely determine the optimal PH_2 control action that is required to regulate the voltage of the stack terminal in the PEMFC model at steady state.
- Develop a neural feedback controller with a one-step-ahead prediction algorithm to track and stabilize the fuel cell system's desired output voltage during the transient state and obtain the best control effort value for the hydrogen partial by employing a multi-objective performance index.

The rest of this paper is structured as follows: In section 2, the PEMFC nonlinear model is presented. Section 3 explains the proposed predictive neural controller design. Section 4 details the simulation results, and section 5 describes the conclusions of this work.

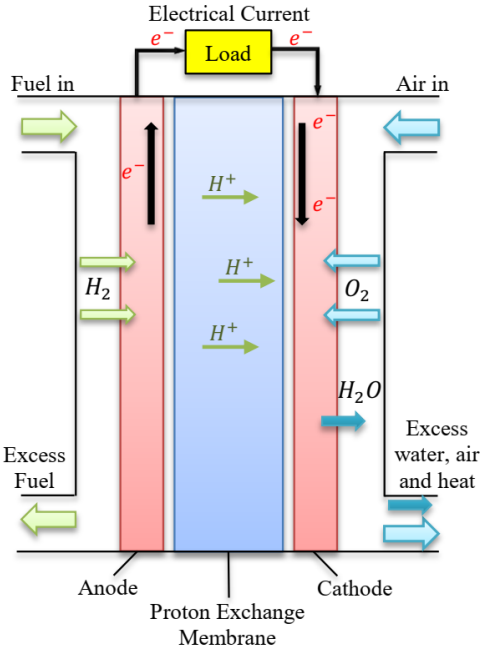

Figure. 1 Proton exchange membrane fuel cell structure

2. PEMFC nonlinear model

PEMFCs use chemical reactions to generate electrical energy without emitting any unwanted byproducts [18]. Fig. 1 shows the structure of the PEMFC model. This particular type of cell relies on a unique, specific polymer membrane covered in extensively dispersed catalyst particles. From the anode side, hydrogen is fed into the membrane, where the catalyst causes the hydrogen atoms to release their electrons and transform into protons H^+ (ions) [4, 15].

The chemical reaction occurring at the anode is as given in Eq. (1) [4, 15]:

$$2H_2 \rightarrow 4H^+ + 4e^- \quad (1)$$

Only H^+ ions move through the proton exchange membrane (PEM), and before they reach the cathode side, the electrons travel to an external circuit to provide the electrical output. The oxygen from the air is mixed with the electrons and hydrogen ions to create water. The chemical reaction occurring at the cathode is illustrated in Eq. (2) [4, 15]:

$$4e^- + 4H^+ + O_2 \rightarrow 2H_2O \quad (2)$$

The overall reaction becomes as described in Eq. (3) [4, 19]:

$$2H_2 + O_2 \rightarrow 2H_2O + \text{electrical energy} \quad (3)$$

Table 1. The physical parameters of the fuel cell [15, 19-21].

Parameters	Values	Units
Ncell	32	--
T	298	K
A	64	cm^2
L	$178 * 10^{-6}$	cm
PH_2	1-5	Bar
PO_2	0.2	Bar
Rc	0.0003	Ω
B	0.0169	Volt
α_1	0.948	Volt
α_2	0.00312	Volt/k
α_3	$7.6 * 10^{-5}$	Volt.K^{-1}. Mol^{-1}/cm^3
α_4	$-1.93 * 10^{-4}$	Volt.K^{-1}/A
J	0.0073	mA/cm^2
Jmax	0.469	mA/cm^2
Φ	23	--

To avoid flooding and rendering the cell inoperable, the created water must be expelled [20]. In this context, a single cell generates between 0.5 and 0.9 under standard operating circumstances. Since a higher power is required, several cells are connected serially as needed to form what is known as a "stack," and a stack arrangement can be as powerful as hundreds of kilowatts under typical operating settings. PEMFCs provide a number of notable advantages, including zero waste material properties and high performance [18, 19]. PEMFCs operate at temperatures ranging from 50 to 100 °C, which permits a quick start-up operation with high efficiency depending on external environmental factors [18]. The polarization curve, which displays highly nonlinear relationships between voltages and current, is typically employed to express the performance of the entire cell [19, 20]. One way to define a single cell's output voltage is as follows [4, 20]:

$$V_{cell} = V_{steady} - V_{transient} \quad (4)$$

$$V_{steady} = E_N - V_{ohm} \quad (5)$$

$$V_{transient} = V_{act} + V_{con} \quad (6)$$

Where V_{cell} is the output voltage of a fuel cell, E_N is the reversible voltage of the fuel cell, V_{ohm} is the ohmic voltage reductions brought on by the resistance to protons' and electrons' passage through the solid electrolyte, V_{act} is the voltage drop brought on by anode and cathode activation, and V_{con} is the voltage drop caused by a decrease in the concentration of the reactants' gases or the passage of mass of oxygen and hydrogen.

It is possible to calculate each term in Eqs. (4-6) using the physical fuel cell characteristics mentioned in Table 1 [15, 19-21]. The ideal output voltage is represented by E_N, which is the cell's electrochemical thermodynamic potential and may be calculated as follows [15, 19]:

$$E_N = 1.229 + 4.3085 \times 10^{-5} \times T \times (\ln PH_2 + 0.5 \ln PO_2) - 0.85 \times 10^{-3} \times (T - 298) \quad (7)$$

Where PH_2 and PO_2 are the partial pressure of hydrogen and the partial pressure of oxygen, respectively and T is the fuel cell temperature expressed in Kelvin (K).

The voltage drop caused by the activation of the anode and cathode is known as the "activation drop voltage," and it can be represented as follows [4, 20]:

$$V_{act} = \alpha_1 + \alpha_1 \times T + \alpha_3 \times T \times \ln CO_2 + \alpha_4 \times T \times \ln I \quad (8)$$

Where α_i are parametric coefficients and CO_2 is the amount of dissolving oxygen in mol/cm^3 of the cathode catalytic surface.

Using Henry's law, CO_2 can be calculated from the oxygen partial pressure and the cell temperature, as given in Eq. (9) [15, 20]:

$$CO_2 = \frac{PO_2}{5.08 \times 10^6 . exp\left[\frac{-498}{T}\right]} \quad (9)$$

The ohmic loss voltage can be calculated using Eq. (10):

$$V_{ohm} = I \times (R_c + R_m) \quad (10)$$

Where R_m is the equivalent resistance of the electron flow and R_c is the proton resistance constant value.

$$R_m = \frac{\rho_m L}{A} \quad (11)$$

Where L represents the polymer membrane's thickness (cm), A is the live cell area (cm^2), and ρ_m is the membrane's specific resistance, which can be calculated using Eq. (12) [21]:

$$\rho_m = \frac{181.6\left[1+0.03\left(\frac{1}{A}\right)+0.062\left(\frac{T}{303}\right)^2\left(\frac{1}{A}\right)^{2.5}\right]}{\Phi-0.634-3\left(\frac{1}{A}\right)exp\left[4.18\left(\frac{T-303}{T}\right)\right]} \quad (12)$$

Where Φ is a variable that controls the humidity.

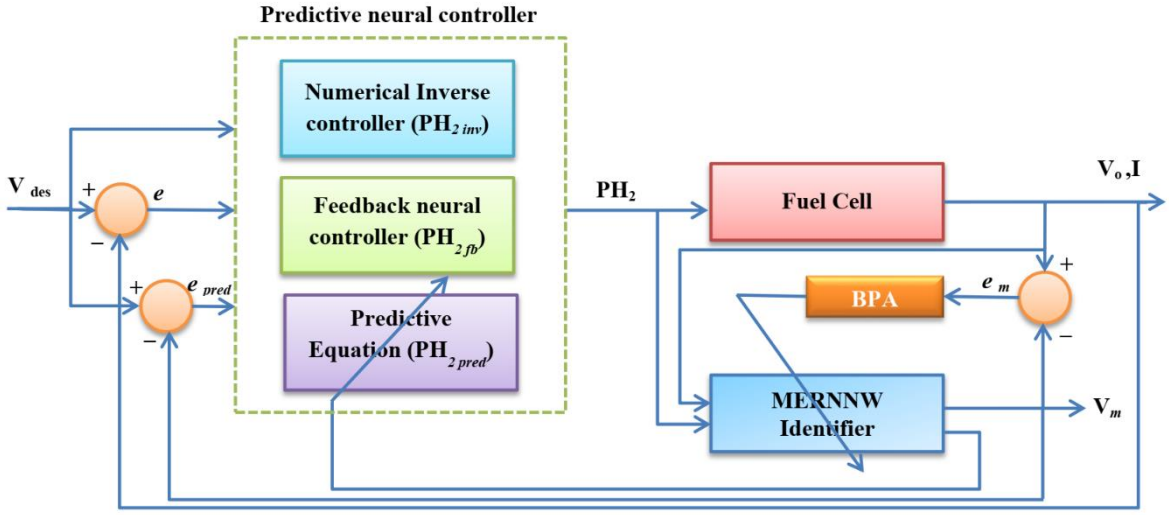

Figure. 2 The proposed predictive voltage control strategy structure

Using Eq. (13) [21], the concentration loss has been determined.

$$V_{con} = -\beta \ln\left(1 - \frac{J}{J_{max}}\right) \tag{13}$$

Where β is a parameter that depends on the cell type, J represents the amount of current that flows through the cell $\left(\frac{A}{cm^2}\right)$, and J_{max} refers to the cell's maximum allowable current density $\left(\frac{A}{cm^2}\right)$. The formula for J_{max} is [15, 20]:

$$J_{max} = \frac{I_{max}}{A} \tag{14}$$

The total output voltage of the stack can be determined by Eq. (15) [19]:

$$V_{FC} = N_{cell} \times V_{cell} \tag{15}$$

Where N_{cell} is the number of cells in the stack.

The fuel cell's overall quantity of power delivered to the load can be calculated as given in Eq. (16) [19]:

$$Power_{FC} = I\ V_{FC} \tag{16}$$

3. Design of predictive voltage controller

The proposed predictive voltage controller for the general form of the PEMFC is depicted in Fig. 2. This controller task is to solve the problem of the fuel cell's output voltage variation while the load current varies and to generate the best value of PH_2, which is fed to the fuel cell to obtain the necessary voltage during variations in the load current.

The first step in the proposed predictive voltage control strategy is the neural network identifier to overcome the difficulty of the mathematical model of the fuel cell in terms of finding the Jacobian function and attaining quick learning without oscillation in the output identifier model. The second step is the feedback neural controller with the numerical feed-forward controller to rapidly and precisely generate the best PH_2 control action required to regulate the voltage of the stack terminal in the PEMFC model at the steady state. The third step is the predictive control law equation with a one-step-ahead prediction algorithm that leads to obtaining the optimal or near optimal value for the hydrogen partial pressure control effort for tracking and stabilizing the fuel cell system's desired output voltage in the transient state.

3.1 Neural network identifier

Modeling and system identification are the primary aims of the proposed controller's structure, which is utilized to provide the preconditions for analysis and controller design. The result of system identification is to find a mathematical model whose output corresponds to the output of a dynamic system for a given input [22, 23]. The recurrent neural network structure is used to construct the neural network identification model of the fuel cell type (PEMFC) system based on the Modified Elman recurrent neural network (MERNN) in order to develop the neural PEMFC model. The MERNN is a partial neural network structure proposed in [24, 25]. Among the different forms of neuronal cells that make up neural networks (NNs), Elman neural networks (ENNs) are a subtype that are built in accordance with specified principles.

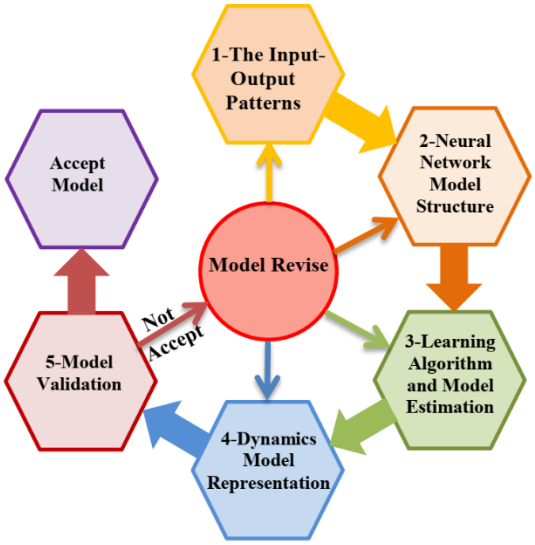

Figure. 3 Modeling and identification procedures for PEMFC systems

In reality, neural networks are the mathematical model that can process data concurrently and has strong fault tolerance, adaptively, and associative memory capabilities [26, 27]. MERNN was chosen over conventional neural networks for the suggested identification because it offers particular benefits. The context units have many orders of the self-connection in the working, which raises the order of the hidden units, these advantages give the proposed identity structure a number of useful properties, such as strong robustness performance, no output oscillation, favorable dynamic properties, and increasing degree of the control performance. The five fundamental steps shown in Fig. 3 are used to overcome the difficulty in identifying and modeling the PEMFC system and to employ artificial neurons as the fundamental building block for the construction of multi-layered and higher-order neural networks to explain the dynamic model of the PEMFC.

According to the operational description of the nonlinear proton exchange membrane fuel cell PEMFC model. The major physical variable outputs of the fuel cell type (PEMFC) model are divided into three types: the first major output is the fuel cell's stack output voltage (V_{FC}); the second one is the variable operational temperature output (T) of the fuel cell model; and the third major is the variability of the output current (I) of the fuel cell. In addition, the PEMFC system's two inputs—the first of which is the controlled effort of the hydrogen partial pressure (PH_2) and the second input is the constant value of the oxygen partial pressure (PO_2), that represented in this work.

The block diagram of the suggested neural network

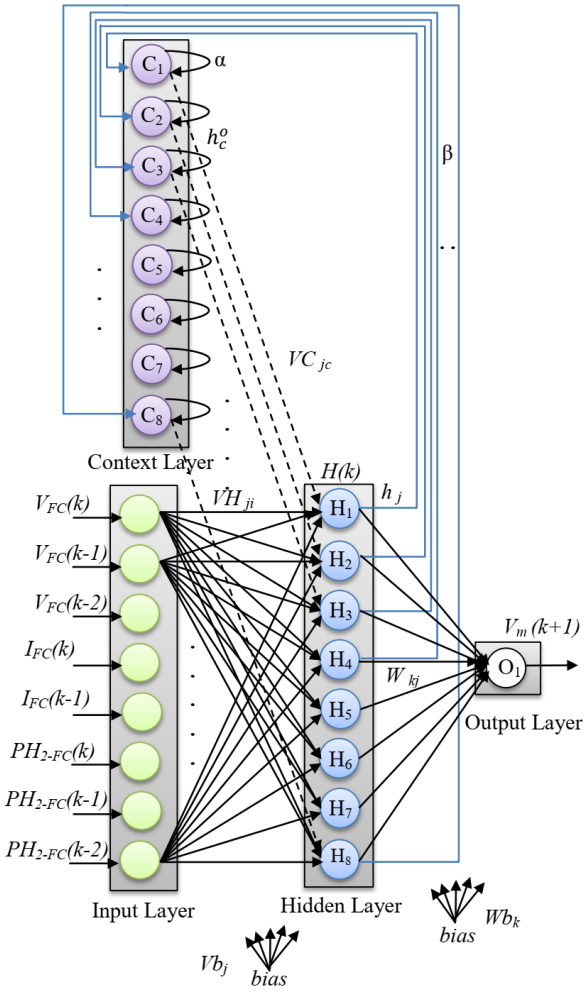

Figure. 4 The structure of the proposed MERNN identifier model

identification for the PEMFC system is shown in Fig. 4. The MERNN's structure consists of four layers, as follows [26, 27]: The input layer: It serves as a buffer by passing the data on without any modification just scaling the values. The second main layer is the hidden layer: It is a functionally active layer that it is based on the non-linear activation function. The third layer is memory layer or the context layer and did not have any activation functions and it is used as storage memory for increasing the speed of the learning networks. The context node's computed value is identical to that of the hidden output node, with the exception that recurrent connections cause it to be one unit later. Both the hidden layer and the context layer have the same number of nodes. The output layer: A linear activation function defines each node of the output layer. The suggested dynamic model of the PEMFC system's Modified Elman recurrent neural network (MERNN) identification is represented in Eq. (17).

$$V_m(k+1) = F_m[V_{FC}(k), V_{FC}(k-1), V_{FC}(k-2), I(k), I(k-1), PH_2(k), PH_2(k-1), PH_2(k-2)] \quad (17)$$

Where V_m is the neural model of the fuel cell's output voltage and $F_m[-]$ refers to the relationship function between the fuel cell system's previous input and output values, representing the (MERNN) model.
The weight definitions of the modified Elman recurrent neural network layers, which are depicted in Fig. 4, are as follows: VH: The hidden layer's weight matrix. VC: The context layer's weight matrix. Vb: The hidden layer's weight one demission vector. W: The output layer's weight matrix. Wb: The output layer's weight one demission vector. O: Stands for a linear node. H: Stands for a nonlinear node with a sigmoid function.

The initial calculation within the neuron is the weighted sum net_j of the inputs, as represented in Eq. (18) [26, 27]:

$$net_j = \sum_{i=1}^{I} VH_{ji} \times G_i + \sum_{c=1}^{C} VC_{jc} \times h_c^o + bias \times Vb_j \quad (18)$$

Where G_i stands for the inputs of the neural network, h_c^o is the memory layer's output, and *I*, *C*, and *j* are denote to how many nodes are in the input layer, the memory layer, and the active hidden layer, respectively.

In the modified Elman network, the output of the c^{th} context unit is provided by Eq. (19) [26, 27]:

$$h_c^o(k) = \alpha h_c^o(k-1) + \beta h_j(k-1) \quad (19)$$

Where $h_j(k)$ is the output of the active hidden unit, α is a gain in the context or memory units as a self connections, and β is the connection weight from the hidden units j^{th} to the context units c^{th} at the context layer. The training process does not change the value of α and β; they are randomly chosen between 0 and 1.

Then, as indicated in Eq. (20), a continuous bipolar activation function named sigmoid is applied at the hidden layer nodes, allowing the output of neuron h_j in the hidden layer to be expressed as given in Eq. (21) [22, 23].

$$H(net_j) = \frac{2}{1+e^{-net_j}} - 1 \quad (20)$$

$$h_j = H(net_j) \quad (21)$$

Additionally, the output layer receives the hidden layer's results after they have been computed. The output layer computes the weighted sum ($neto$) of its inputs using one linear neuron, as detailed in Eq. (22) [22, 23]:

$$neto_k = \sum_{j=1}^{J} W_{kj} \times h_j + bias \times Wb \quad (22)$$

Where W_{kj} is the output layer's weight matrix and $\overrightarrow{Wb}$ is the output neuron's weight vector.

The output neuron response comes from the output layer is utilized to determine the output response of the proposed model (identifier model) based on neural networks that represents the voltage of the fuel cell. The result ($neto_k$) is then passed by the linear neuron through a linear function (*L*), as depicted in Eq.(23), which models the output voltage of a FC:

$$O_k = L(neto_k) = V_m \quad (23)$$

Where V_m denotes the fuel cell output modeling voltage and a linear function is L(x) = x with a slope of one in this case.

To learn the weights of the identifier model (modified Elman recurrent neural networks) and to update the weights of the networks, the back-propagation algorithm is used with the cost function (mean square error), which represents the average sum of the squares of the differences between the desired outputs (V_{des}) and network outputs(V_{FCM}), is used to evaluate the model's performance:

$$E = \frac{1}{K}\sum_{i=1}^{K}\left(e_m(k+1)\right)^2 \quad (24)$$

$$E = \frac{1}{K}\sum_{i=1}^{K}(V_{FC}(k+1) - V_m(k+1))^2 \quad (25)$$

Where K is the number of patterns in the training set overall and E is the objective cost function.

After utilizing the neural network's training procedure, as depicted in Fig. 4, then applying the back-propagation learning algorithm for reducing the error of the output voltage model (neural network model) V_m, and the real output voltage V_{FC} which is almost equal to zero, the identifier model based on MERNN will produce the same actual output voltage response. Therefore, it will be possible to use a testing set to verify that the model's output voltage matches the desired fuel cell voltage that describes the variation between the reference voltage and the fuel cell identity model output voltage, as well as to verify that the network is perfectly learned. The series-

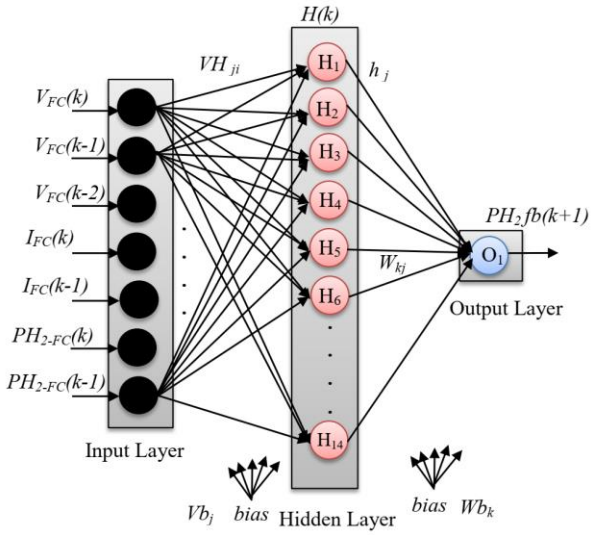

Figure. 5 The proposed MLP neural controller structure

parallel identification model is created using the modified Elman neural network, for which it is evident that at each instant of time, the Fuel-Cell system's previous inputs and outputs are fed into the network, and the output of the network returns the prediction error. However, the inputs to the neural network (identifier) model in the structure are the outputs of the real fuel cell PEMFC model, this technique can only be used in combination with the series-parallel system.

3.2 The feedback neural control design

In general, when the output voltage of the fuel cell type (PEM) system deviates from the required input voltage during the transient state, the feedback controller is crucial to preserving the tracking voltage error of the fuel cell system. In addition, this controller finds the optimal hydrogen partial pressure feedback control action ($PH_{2\,fb}$) that makes the feedback voltage error as small as possible. Specifically, this controller is based on a multilayer perceptron neural network. Fig. 5 demonstrates the proposed neural network controller structure. Particularly, the structure of the MLP neural network consists of three layers [22, 23]. The input or buffer layer consists of seven linear input neurons; these inputs are the present and previous inputs of the desired fuel cell voltage, current, and hydrogen partial pressure, as depicted in Fig. 5.

The hidden layer is composed of 14 neurons with a nonlinear activation function. The output layer consists of a single linear neuron that represents the hydrogen feedback control action. The neural network was trained using the back-propagation learning algorithm. The performance index to be minimized is given below:

$$J = \frac{1}{2}\sum_{k=1}^{K}\left(PH_{2\,ref}(k) - PH_{2\,fb}(k)\right)^2 \quad (26)$$

Where $PH_{2\,ref}(k)$ is the hydrogen partial pressure's reference control action, $PH_{2\,fb}(k)$ is the hydrogen partial pressure feedback control action, and K denotes the number of patterns.

The numerical feedforward controller (NFFC) can be used to determine the $PH_{2\,ref}$, and it is expected that the NFFC will determine the inverse dynamics of the PEMFC system, hence the name "Inverse feedforward controller" (IFC). The appropriate input hydrogen partial pressure for the feedback controller is likewise created using the NFFNC. In this regard, several equations need to be numerically determined in order to achieve this controller, as follows:

$$V_{des} = N_{cell}(E_N - V_{ohm} - V_{act} - V_{con}) \quad (27)$$

$$E_N = 1.229 - 0.85 \times 10^{-3}(T - 298) + 4.3085 \times 10^{-5} \times \ln PH_{2\,ff} + 0.5 \ln PO_2 \quad (28)$$

Then, combining Eq. (27) with Eq. (28) leads to providing $PH2_{ref}$ as in Eq. (29).

$$PH2_{ref} = ln^{-1}\frac{\left(\frac{V_{des}}{N_{cell}}\right) + V_{act} + V_{ohm} + V_{con} - 1.229 + \left(0.85 \times 10^{-3}\right)(T - 298)}{(4.3085 \times 10^{-5})} - 0.5 \times ln(PO_2) \quad (29)$$

Where V_{des} is the required input voltage for the feedback controller.

The initial stage in calculating the hydrogen feedback $PH_{2\,fb}$ control action is calculating the input's weighted sum $netj$ as in Eq. (30):

$$net_j = \sum_{i=1}^{I} VH_{ji} \times D_i + bias \times Vb_j \quad (30)$$

Where VH_{ji} indicates the hidden layer's weight matrix, D_i denotes the controller's input vector, and I and J reflect that how many nodes in the input layer and the hidden layer, respectively.

Furthermore, the sigmoid activation function shown in Eq. (31) is applied to the hidden nodes. As a result, Eq. (32) can be used to express the output of neuron h_j in the hidden layer.

$$H(net_j) = \frac{2}{1 + e^{-net_j}} - 1 \quad (31)$$

$$h_j = H(net_j) \quad (32)$$

The results of the hidden layer are subsequently computed and fed to the output layer, which utilizes one linear neuron for summing the weighted of the output layer ($neto_k$) depend on its inputs values, as shown in Eq. (33):

$$neto_k = \sum_{j=1}^{J} W_{kj} \times h_j + bias \times Wb \quad (33)$$

Where W_{kj} represents the output layer's weight matrix and Wb is the one dimension vector of the output neuron's weight.

The suggested neural network controller's output ($neto_k$) is determined by a single linear function (L) neuron in the output layer, which then represents the hydrogen control action of the fuel cell, as illustrated in Eq. (34):

$$O_k = L(neto_k) = PH_{2fb} \quad (34)$$

For modifying the weights of the MLP neural network, the back-propagation algorithm is used for the proposed feedback MLP controller. In particular, the weights of the connection matrix between the hidden layer and the output layer (W_{kj}) are updated as follows:

$$W_{kj}(k+1) = W_{kj}(k) + \Delta W_{kj}(k) \quad (35)$$

$$\Delta W_{kj}(k) = \eta\, h_j\, e_k \quad (36)$$

$$e_k = PH_{2\,ref}(k) - PH_{2\,fb}(k) \quad (37)$$

Where η is the learning rate and e_k represents the difference between the reference value the actual neural output for hydrogen partial pressure.

The following expression is the weight update for the connection matrix between the hidden layer and the input layer (VH_{ji}):

$$VH_{ji}(k+1) = VH_{ji}(k) + \Delta VH_{ji}(k) \quad (38)$$

$$\Delta VH_{ji}(k) = \eta f(net_j)'\, D_i \sum_{k=1}^{K} e_k\, W_{kj} \quad (39)$$

The suggested controller will be able to produce feedback hydrogen control actions for PEMFC systems after being trained. A testing (input-output) set will be utilized to describe the convergence between the (PH2ref) reference value, which can be determined from the proposed numerical feedforward neural controller (NFFNC), and the neural output for PEMFC, in order to verify and confirm that the neural network is correctly learned and trained. This will ensure that all of the proposed controller's output values follow the desired values accurately.

3.3 Predictive control law equation

A predictive control law equation is used to predict the hydrogen partial pressure control signal for N steps ahead ($PH_{2\,pred}$). Here, the on-line identifier neural network is used to retrieve the predicted output voltage values for many steps ahead predictive. Rather than carrying out the actual PEMFC model for many steps predictive that lead to determining the predicted values for the hydrogen partial pressure control action by minimizing the multi-objective cost function given in Eq. (40).

$$E_{pred} = \frac{1}{2} \sum_{k=1}^{N} \Big[Q(V_{des}(k+1) - V_m(k+1))^2 + R\big(PH_{2\,ref}(k) - PH_2(k)\big)^2 \Big] \quad (40)$$

Where $PH_2(k)$ is the overall hydrogen partial pressure control signal, $V_{des}(k+1)$ refers to the reference voltage of the fuel cell as output desired, Q and R indicate the coefficients of the control law equation, and N denotes prediction steps ahead.

Consequently:

$$PH_{2\,ref}(k) = PH_{2\,inv}(k) \quad (41)$$

$$PH_2(k) = PH_{2\,inv}(k) + PH_{2\,fb}(k) + PH_{2\,pred}(k) \quad (42)$$

When Eq. (41) and (42) are inserted in Eq. (40), E_m will be provided as in Eq. (43):

$$E_{pred} = \frac{1}{2} \sum_{k=1}^{N} \Big[Q(V_{des}(k+1) - V_m(k+1))^2 + R\Big(PH_{2\,ref}(k) - \big(PH_{2\,inv}(k) + PH_{2\,fb}(k) + PH_{2\,pred}(k)\big)\Big)^2 \Big] \quad (43)$$

$$E_{pred} = \frac{1}{2} \sum_{k=1}^{N} \Big[Q(V_{des}(k+1) - V_m(k+1))^2 + R\big(PH_{2\,fb}(k) + PH_{2\,pred}(k)\big)^2 \Big] \quad (44)$$

This multi-objective performance index will force the output voltage to follow the desired input voltage and force the hydrogen partial pressure to be controlled in the transient period as closely as possible to the reference control signal of the hydrogen partial

pressure by reducing the cumulative voltage error for N steps ahead. The determined control signal of the hydrogen partial pressure will be optimal or near optimal value with regard to the specified values for the control law parameters variables *Q* and *R* because of the convergence of the prediction error E_{pred} is based on the two positive parameters *Q* and *R*. In this context, engineering judgment is used to make the selection of *Q* and *R*, which is frequently done iteratively by comparing the system response to certain design criteria like overshoot and rising time [28]. Additionally, to get the identifier's output voltage $V_m\,(k)$, as near as the fuel cell PEMFC output value $V_{FC}\,(k)$, online identification is required. In order to track any potential changes in the output voltage of the PEMFC system, the MERNN is utilized as an identifier, and the weights of the obtained identifier are modified on-line. The back-propagation algorithm (BPA) is employed to modify the weights of the identifier neural network so that it learns the dynamic behaviour of the fuel cell type (PEM) system using a straightforward gradient descent method. As a result, it can be stated that $V_m\,(k) \approx V_{FC}\,(k)$ and the cost function in Eq. (44) can be expressed as in the proposed Eq. (45):

$$E_{pred} = \frac{1}{2}\sum_{k=1}^{N}\left[Q\left(e_{pred}\,(k+1)\right)^2 - R\left(PH_{2\,fb}\,(k) + PH_{2\,pred}\,(k)\right)^2\right] \quad (45)$$

$$e_{pred}\,(k+1) = V_{des}(k+1) - V_m\,(k+1) \quad (46)$$

In this section, the predictive control action based on one-step ahead of the hydrogen partial pressure $PH_{2pred}\,(k+1)$ will be driven as follows, where N=1:

$$PH_{2pred}(k+1) = PH_{2pred}(k) + \Delta PH_{2\,pred}(k) \quad (47)$$

The proposed predictive control law equation is created by minimizing the quadratic cost function for Eq. (45) in the manner described as follows:

$$\Delta PH_{2\,pred}(k) = -\eta\,\frac{\partial E_{pred}}{\partial PH_{2\,pred}(k)} \quad (48)$$

Eq. (49) is obtained by substituting Eq. (44) into Eq. (48), where the weight space is represented by the usage of the minus sign using gradient-descent, which also shows the search for the weight change's direction and lowers the value of E_{pred}. According to the chain rule distinction, it has:

$$-\eta\,\frac{\partial E_{pred}}{\partial PH_{2\,pred}(k)} = -\eta\,\frac{\partial \frac{1}{2}Q(V_{des}(k+1)-V_m\,(k+1)\,)^2}{\partial PH_{2\,pred}(k)} - \eta\,\frac{\partial \frac{1}{2}R\left(\left(PH_{2\,fb}\,(k)+PH_{2\,pred}\,(k)\right)\right)^2}{\partial PH_{2\,pred}(k)} \quad (49)$$

$$\Delta PH_{2\,pred}(k) = \eta Q\; e_{pred}\,(k+1) \times \frac{\partial V_m(k+1)}{\partial PH_{2pred}(k)} - \eta\; R\;[PH_{2fb}(k) + PH_{2pred}(k) \quad (50)$$

From the modified Elman neural network identifier depicted in Fig. 4, Eq. (50) is solved as follows:

$$\frac{\partial V_m(k+1)}{\partial PH_{2pred}(k)} = \frac{\partial V_m(k+1)}{\partial O} \times \frac{\partial O}{\partial net_o} \times \frac{\partial net_o}{\partial h_j} \times \frac{\partial h_j}{\partial net_j} \times \frac{\partial net_j}{\partial PH_2(k)} \times \frac{\partial PH_2(k)}{\partial PH_{2pred}(k)} \quad (51)$$

In the case of the output having a linear activation function, Eq. (51) becomes as follows:

$$\frac{\partial V_m(k+1)}{\partial PH_{2pred}(k)} = \frac{\partial net_o}{\partial h_j} \times \frac{\partial h_j}{\partial net_j} \times \frac{\partial net_j}{\partial PH_2(k)} \times \frac{\partial PH_2(k)}{\partial PH_{2pred}(k)} \quad (52)$$

$$\frac{\partial V_m(k+1)}{\partial PH_{2pred}(k)} = \frac{\partial net_o}{\partial h_j} \times \frac{\partial h_j}{\partial net_j} \times \frac{\partial net_j}{\partial PH_2(k)} \quad (53)$$

From Fig. 4, the $PH_2(k)$ is linked at node number six to the exciting nodes $VH_{\,j6}$; therefore:

$$\frac{\partial V_m(k+1)}{\partial PH_{2pred}(k)} = \sum_{j=1}^{nh} w_{6j}\; f'\left(net_j\right) VH_{j6} \quad (54)$$

$$\Delta PH_{2\,pred}(k+1) = \eta\; Q\; e_{pred}\,(k+1) \times \left[\sum_{j=1}^{nh} w_{6j}\; f'\left(net_j\right) VH_{j6}\right] - \eta\; R\;\left[PH_{2fb}(k) + PH_{2pred}(k)\right] \quad (55)$$

Where nh represents the number of nodes in the hidden layer.

When Eq. (55) is substituted for Eq. (47), the proposed predictive control law equation of the nonlinear fuel cell model is provided for the one-step ahead prediction, as represented in Eq. (56) in order to obtain the optimal or near-optimal value for the hydrogen partial pressure control effort.

$$PH_{2pred}(k+1) = PH_{2pred}(k) + \eta\; Q\; e_{pred}\,(k+1) \times \left[\sum_{j=1}^{nh} w_{6j}\; f'\left(net_j\right) VH_{j6}\right] - \eta\; R\;\left[PH_{2fb}(k) + PH_{2pred}(k)\right] \quad (56)$$

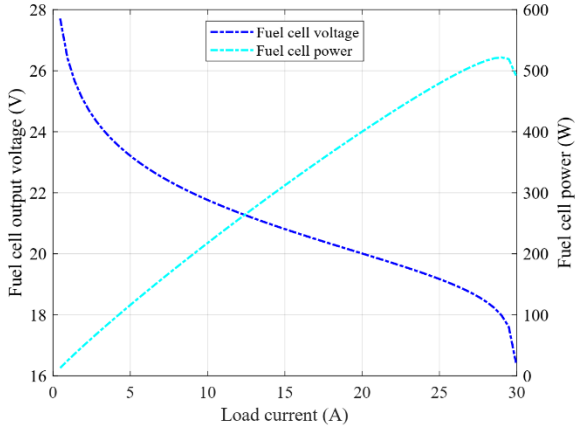

Figure. 6 The stack output voltage and power against the current

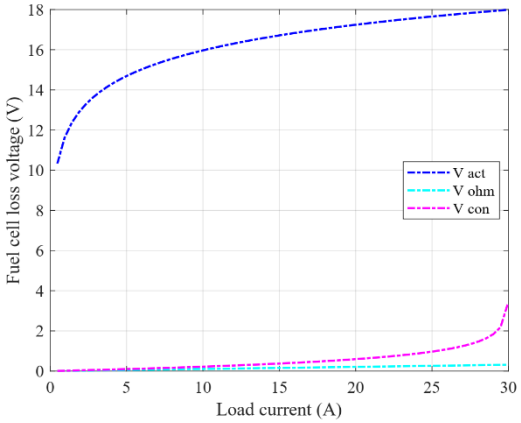

Figure. 7 Fuel cell voltage drop against load current

This control effort will track and stabilize the fuel cell's output voltage model at the desired output voltage in the two states, the transient state and the steady-state of operation.

4. Simulation results

Predictive neural voltage control, as seen in Fig. 2, was used to enhance the performance of the output voltage of the nonlinear PEMFC system. This can be accomplished by regulating the PEMFC output voltage in the presence of current variation and by forecasting the best hydrogen partial pressure (PH_2) values to protect the fuel cell membrane from damage in such a way that extends the fuel cell lifetime without consuming a lot of PH_2. The MATLAB R2020a package and Intel Core i5-1035G4 computer hardware with RAM size is eight Gbye and the clock speed of CPU is equal to 1.50 GHz that were used to validate and construct the proposed controller.

At the controller design's initial stage, study and analysis of the PEMFC system's dynamic properties in relation to its physical parameters, as shown in Table 1, are required to show the nonlinear dynamic

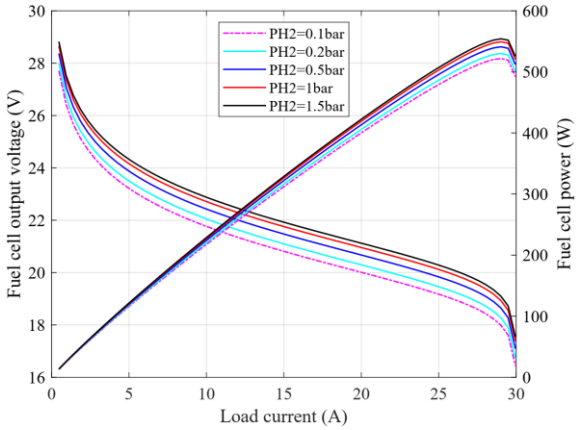

Figure. 8 The maximum power and the output voltage against load current with variable hydrogen partial pressure

behavior of the fuel cell model. In the first analysis: the magnitude of the fuel cell's output voltage and maximum output power response are shown in Fig. 6, where the normal operating conditions of the fuel cell model are (1) the value of the hydrogen partial pressure is equal to 0.1 bar, (2) the value of the oxygen partial pressure is equal to 0.2 bar, (3) the operating temperature of the fuel cell model is equal to 25 °C, under the load current of the fuel cell is variable between 0 and 30 A,

This model's maximum power is obvious at the current equivalent to 29 A. Fig. 7 depicts the loss voltage response of the fuel cell system when the variable load current, which is changeable between 0 A and 30 A. To demonstrate the impact of the hydrogen partial pressure as shown in Fig. 8 as the second study that it variations between 0.1 bar and 1.5 bar and to show the effect on the fuel cell's output voltage as well as the maximum output power can be the fuel cell operated during the load current varies between 0 A and 30 A. But the operating temperature of the fuel cell is constant at 25 °C.

The fuel cell's output voltage grows as the hydrogen partial pressure increases, as shown in Fig. 8. As a result of the PEMFC system's increased thermodynamic potential (EN) value, as shown in Eq. (7), the dynamic performance of the output voltage of the fuel cell system has improved.

The impact of temperature fluctuations of the fuel cell system is studied as shown in Fig. 9, where the temperature is changing from 25 °C to 85 °C during the load current of fuel cell is variable from 0 A to 30 A, while the partial pressures of hydrogen and oxygen are constant at 1.0 bar and 0.2 bar, respectively. The output voltage of the (FC) grows as the temperature rises. The PEMFC system's EN value has been enhanced to increase and decrease the parameter

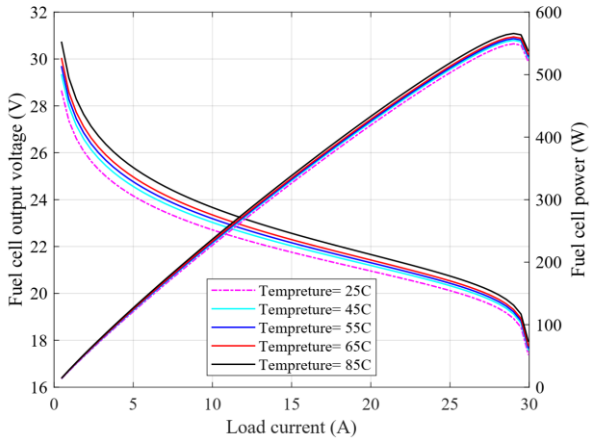

Figure. 9 The stack output voltage and power against load current with temperature

impact values on the loss voltage, which has improved the performance of the fuel cell system. However, when the temperature rises, the fuel cell will operate with less of the required humidity for the membranes, which will shorten the fuel cell's lifetime.

The first stage in developing the proposed controller design is to determine the neural network PEMFC model (system identification), which employs the identification algorithm's five steps, as depicted in Fig. 3. To create input-output patterns as the first step, as shown in Fig. 10 that will stimulate and excite all nonlinear sections of the dynamic behaviour of the fuel cell system.

In step two, the PEMFC system model is displayed using the structure of recurrent neural network based on Modified Elman recurrent neural networks that it described in Fig. 4. Accordingly, the suggested number of nodes for each of the four layers—the input layer, the context layer, the hidden layer, and the output layer—is as follows: [8: 8: 8: 1]. The third step involves learning the neural network identifier model off-line using the back-propagation algorithm and then tuning the model online. The fourth step is to represent the proposed the order of the dynamic model of the FC type (PEM) system, which is based on the equation of the stack output voltage of the PEMFC system that it given in Eq. (17), which has the third-order dynamic behavior. In order to resolve the numerical problems related to actual values, the signals entering or leaving neural network (NN) has been treated to lie between (-1) to (+1). Given that the patterns of the inputs (load currents of 1 to 25 A and hydrogen partial pressures of 1 to 5 bars) and the outputs (20 to 28 volts) are both greater than 1, scaling functions must be applied at the first layer and last layer of neural network terminals (input-output), respectively, as shown in Figs. 10 (a) and (b) to convert scaled values to actual values and

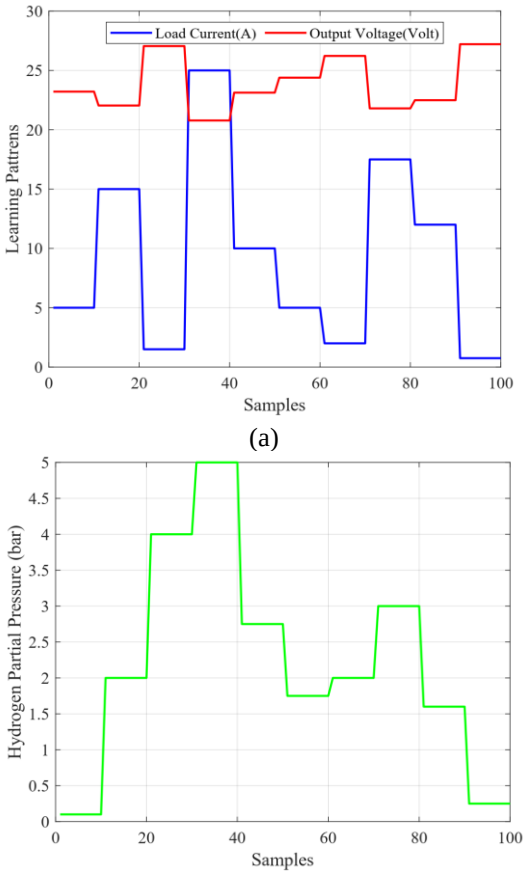

Figure. 10 The PEMFC model's neural network identification learning set: (a) Output voltage and load current, and (b) The input of partial pressure of hydrogen

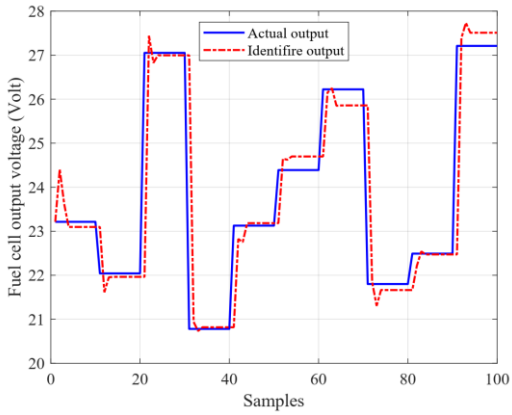

Figure. 11 Learning response for the MERNN identifier

vice versa. In the learning mode, the real output voltage of the FC system model is shown in Fig. 11, with a model error of zero approximation for 100 patterns, which highlights the good responsiveness of the neural network identifier for the PEMFC model.

The performance of the mean square error (objective function) is depicted in Fig. 12 and is based on the off-line back-propagation learning algorithm. It has the minimum performance index value that

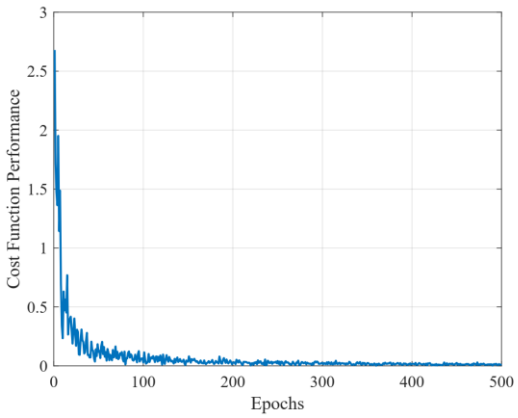

Figure. 12 The proposed controller's performance index during the learning process

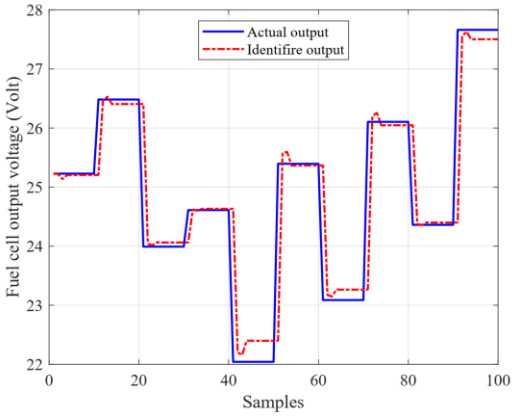

Figure. 13 Testing response for the MERNN identifier

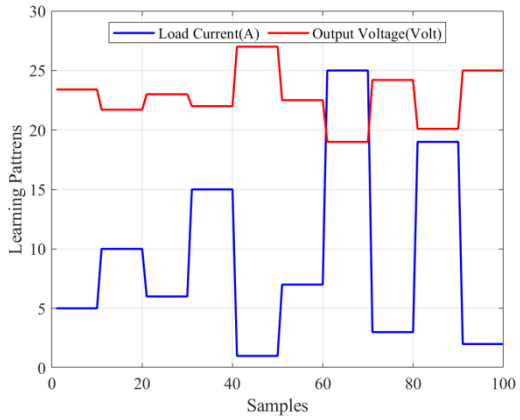

Figure. 14 The MLP neural network controller's learning set (voltage and load current)

reaches 0.0134 during 500 epochs. The fifth step, model validation, is accomplished by testing the neural network identifier PEMFC model with 100 new patterns. As shown in Fig. 13, the PEMFC model identifier of the neural networks' answers matched the real output voltage of the fuel cell, and the overlearning issue that arises during the BP method's learning cycle was not a problem.

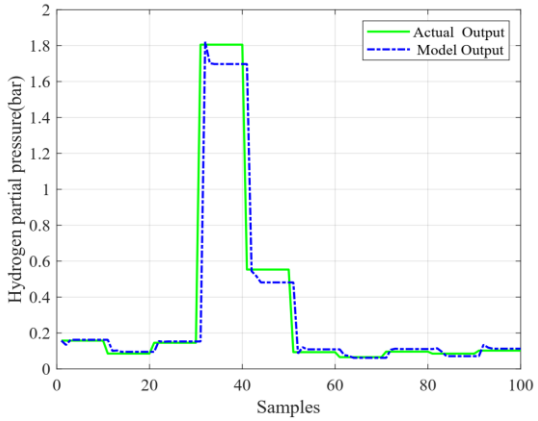

Figure. 15 Learning response of the MLP neural network controller

The MLP neural controller receives 100 samples as an input (hydrogen partial pressure and load current) and an output (voltage), as illustrated in Fig. 14.

As indicated in Fig. 5, which demonstrates the structure of the feedback MLP neural network controller, the suggested number of neurons nodes for the input layer, hidden layer, and output layer are as follows: [7:14:1]. Fig. 15 illustrates the learning response for the MLP neural network controller, based on Eq. (34), which was learned using the back-propagation learning algorithm.

The second stage involves the design of the neural feedback controller, which can be carried out using the MLP neural network and mean square error (objective function). At this stage, the proposed numerical feed-forward neural controller (NFFNC) design must be used to calculate the reference (PH_{2ref}) control action, which it is based on Eq. (29) in order to keep the output voltage of the fuel cell at the desired voltage and the tracking voltage error become zero value at steady-state. Fig. 16 shows the response of the actual output voltage of the PEMFC system when we applied the feedback MLP neural controller. Although the control action tried to track and follow the desired output voltage for the ten different step-changes, but the output voltage response at steady state has error and it is not equal to zero, and there is an oscillation in the output. Consequently, the one-step-ahead predictive controller will be incorporated to enhance the fuel cell's performance, which can be implemented using the multi-objective cost function and the neural network identification PEMFC model based on Eq. (56). Fig. 17 demonstrates the one step ahead prediction response of the (PH_2) control action of the proposed predictive neural controller. The ideal response of the (PH_2) control action includes the best value, fast and smooth control action to follow the

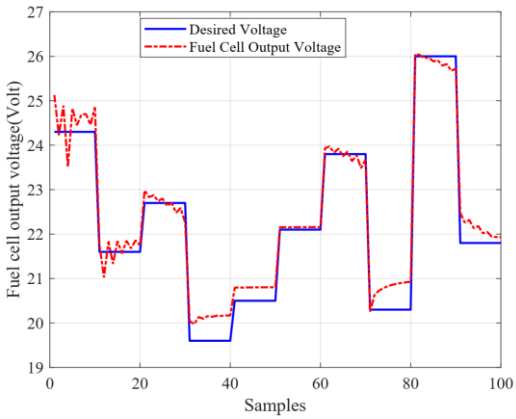

Figure. 16 The actual output voltage for the feedback neural controller

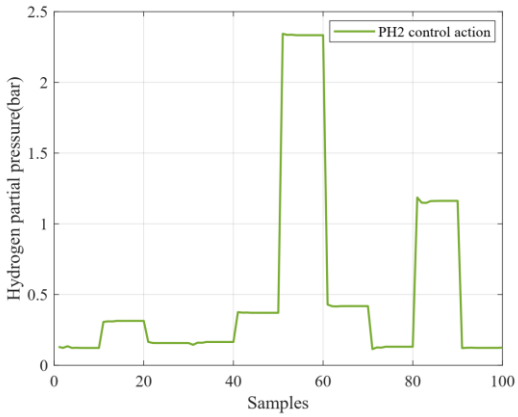

Figure. 17 The response for the one-step-ahead prediction control action PH_2

target output voltage of the PEMFC system, which roughly minimizes the transient state and the steady-state deviation from zero when the Q and R parameters are taken to be 0.085 and 0.01, respectively.

Fig.18 demonstrates the PEMFC system's actual output voltage for the one-step-ahead predictive neural controller. From this figure, it is clear that the response is fast and smooth to track the desired output voltage of the fuel cell model.

By analyzing and contrasting the PEMFC system under random current variations and the minimum voltage tracking error, we were able to compare the numerical simulation results of the proposed controller with those of other types of controllers based on improving system performance in terms of quickly and precisely tracking the desired voltage and consuming less energy. The numerical comparison of the proposed controller with various types of controllers is displayed in Table 2. The proposed controller was first contrasted with the work in [20], which suggested a neural predictive controller with CPSO to ascertain the hydrogen partial pressure

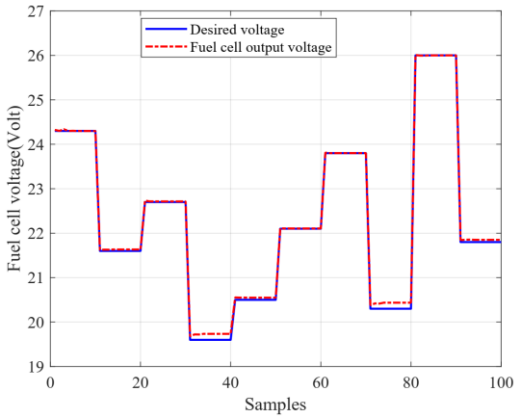

Figure. 18 PEMFC system's actual output voltage for the one-step-ahead predictive voltage controller

Table 2. The numerical comparison of the proposed controller with various types of controllers

Type of Controller	Algorithm	Voltage Error	Oscillation
Predictive neural controller 1-10 step ahead [20]	CPSO (Off-line)	0.08	±0.05
NARMA-L2 inverse neural controller [15]	FF	0.09	±0.17
	CPSO	0.083	±0.12
	FFCPSO (On-line)	0.055	±0.1
The proposed predictive control law equation	BPA (On-line)	0.01	No oscillation

action to adhere to the desired output voltage of the PEMFC system during changes in the load current.

Fig. 19 shows the PEMFC system's actual output voltage for the input set taken from [20] and applied to our proposed controller. The optimal response will be attained for one-step ahead. The voltage tracking error was decreased from 0.08 to 0.01 volt, and enhancement of the tracking voltage error by 87.5%. The oscillation was entirely erased, and a smooth hydrogen partial pressure control action was generated. Although the PEMFC system's actual output voltage in [20] could track the desired output for one-step-ahead prediction for five different load current step-changes with small output oscillation, the voltage error was not equal to zero at steady state, it caused overshoot response in the start sample, and the response of the control action (hydrogen partial pressure) was not smooth. However, in order to improve the reaction and overcome the limitations of the one-step forward response, the authors took 10

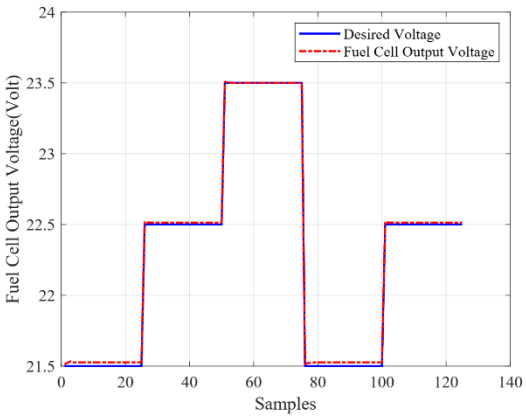

Figure. 19 PEMFC system's actual output voltage for the input set from [20]

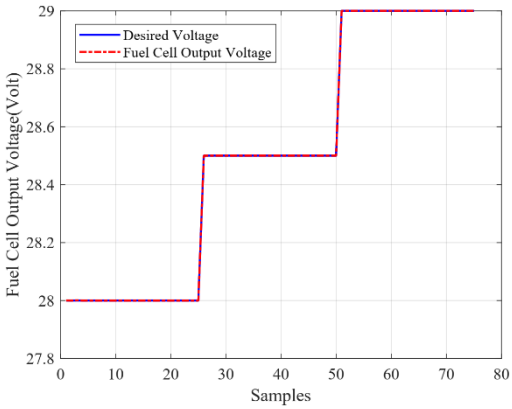

Figure. 20 PEMFC system's actual output voltage for the input set from [15]

steps ahead in [20] to reach the best response, which resulted in a slower response with more processing time.

Therefore, the proposed predictive neural controller resulted in better control performance because it generated the optimal or near-optimal control action based on the predictive control law equation with the neural network identifier as a guide. While in [20], the PH_2 control action was generated based only on the feedback neural controller. Generally, the proposed predictive controller is utilized to predict the ($PH_{2\ pred}$) control action depending on the MERNN identifier, which has a context layer that serves as memory and aids in providing good dynamic characteristics, high order control performance, and self-connection of the memory units that raise the order of the active neurons at hidden units. On the other hand, the controller in [20] relies on a traditional MLP identification model, which consists of [5:7:1] nodes, comprising five nodes for the input layer, seven nodes for the hidden layer, and one node for the output layer. The suggested predictive controller, however, relies on the MERNN identifier network, which consists of [8:8:8:1] nodes, including eight nodes for input, context, and hidden layers, and one node for output layer. Furthermore, in the proposed controller, when the PEMFC's output voltage deviates from the desired input voltage during a transient condition, the feedback controller is utilized to maintain the voltage error at steady state at zero value of the fuel cell model. In addition, the proposed method determines the best hydrogen partial pressure feedback control action ($PH_{2\ fb}$) to minimize the feedback voltage error. The difference between the structure of the proposed controller and the structure of the controller in [20] is the type of the identification networks and their structures. In addition, compared to the controller in [20], the suggested predictive voltage controller offers outstanding learning to provide the optimal control action to follow the desired voltage and achieve the target voltage point without oscillation and with the least amount of tracking voltage error. This control accuracy is achieved because there are more sub-controllers that control the PH_2 control action compared to the controller in [20]. As a second comparative study, we compared the suggested predictive methodology with the results in [15], which introduced the neural network NARMA-L2 structure model and the hybrid (FF-CPSO) firefly-chaotic particle swarm optimization algorithm that used to build the model and control system for the nonlinear PEMFC model. The purpose of the research in [15] was to find the PH_2 control action that regulates the nonlinear PEMFC system's output voltage only at steady-state. Regardless of whether the fuel cell output voltage follows and tracks the desired voltage, there was an oscillation in the output. However, if the same input that has been taken from [15] is applied to our proposed controller, the optimal response will be achieved, where the voltage error is reduced from 0.055 volts to 0.01 volts, and enhancement of the tracking voltage error by 81.8%. The oscillation effect is completely eliminated. Fig. 20 shows the PEMFC system's actual output voltage for the input set that has been taken from [15].

This superiority was attained because the proposed predictive neural controller generates the control action based on both the predictive control law equation and the feedback neural controller. While in [15], the controller generated the control action depending only on the inverse neural controller, which gives a good response in the steady state but generates errors in the transient state. In addition, the identifier model used in [15] is based on a conventional MLP neural network structure. While the identifier model for our proposed controller is

based on the MERNN structure. Specifically, the MERNN provides more accurate identification results because it has an additional context layer that serves as memory and aids in good dynamic characteristics, high order control performance, and self-connection of the memory units that raise the order of the hidden unit in the structure of the neural model identifier. Finally, the simulation results show that the proposed predictive neural network controller can produce the optimal hydrogen partial pressure control action, enabling the fuel cell to track the required voltage with the lowest tracking errors and achieve optimal performance without oscillation in the output voltage of the fuel cell.

5. Conclusions

The development of a predictive neural controller to enhance the performance of the nonlinear PEMFC model by controlling the output voltage of the FC stack terminal during variable load current has been proposed in this paper. To solve the problem of the output voltage variation from the fuel cell with varying the load current, which is regarded as a critical problem in the nonlinear fuel cell behavior, we proposed the predictive controller that consists of an identifier neural network (MERNN) with a back-propagation algorithm, a feedback neural controller based on the MLP, and a predictive control law equation.

This controller has the following capabilities that are provided from the simulation results as follows:

- It overcomes the difficulty of the mathematical model of the fuel cell in terms of finding the Jacobian function and attaining quick learning without oscillation in the output neural model identifier.
- It determines the optimal hydrogen partial pressure control action (PH_2) value in order to improve the dynamic performance of the nonlinear fuel cell output voltage and stabilize it at the desired voltage.
- It generates the optimal or near-optimal value of PH_2 required to supply the necessary output voltage during variations in the load current and reach the desired voltage at the minimum time.
- A one-step-ahead prediction-control law equation led to tracking and stabilizing the fuel cell system's desired output voltage during transient and steady states.
- The tracking voltage error of the fuel cell is approximately equal to zero and without oscillation in the output voltage.

For future research, we recommend that the experimental setup of the suggested predictive control technique be implemented using the LabVIEW package.

Conflicts of interest

There are no potential conflicts based on the authors.

Author contributions

Fatima Abdul Sattar AL-Taie and Ahmed Sabah Al-Araji developed the predictive neural controller for the nonlinear fuel cell system. Fatima Abdul Sattar AL-Taie described the proposed predictive control law. Ahmed Sabah Al-Araji explained the mathematical model of the fuel cell. Fatima Abdul Sattar AL-Taie and Ahmed Sabah Al-Araji demonstrated the simulation results of this research.

References

[1] O. Belounis and H. Labar, "Fuzzy Sliding Mode Controller of DFIG for Wind Energy Conversion", *International Journal of Intelligent Engineering and Systems*, Vol. 10, No. 2, pp. 163-172, 2017, doi: 10.22266/ijies2017.0430.18.

[2] J. Zhu, P. Zhang, X. Li, and B. Jiang, "Robust Oxygen Excess Ratio Control of PEMFC Systems using Adaptive Dynamic Programming", *Energy Reports*, Vol. 8, No. 1, pp. 2036-2044, 2022.

[3] N. H. Jawad, A. A. Yahya, A. R. A. Shathr, H. G. Salih, K. T. Rashid, S. A. Saadi, A. A. AbdulRazak, I. K. Salih, A. Zrelli, and Q. F. Alsalhy, "Fuel Cell Types, Properties of Membrane, and Operating Conditions: A Review", *Sustainability*, Vol. 14, No. 14653, pp. 1-49, 2022.

[4] A. Djerioui, D. Ouali, and M. Ladjal, "Sliding Mode Control Using SVM for Power Quality Enhancement in Stand-Alone System Based on Four-Leg Voltage", *International Journal of Intelligent Engineering and Systems*, Vol. 11, No. 2, pp. 266-274, 2018, doi: 10.22266/ijies2018.0430.29.

[5] C. Damour, M. Benne, B. G. Perez, and J. P. Chabriat, "Neural Model-Based Self-Tuning PID Strategy Applied to PEMFC", *Engineering*, Vol. 6, No. 4, pp. 159-168, 2014.

[6] Y. Budak, and Y. Devrim, "Investigation of Micro-Combined Heat and Power Application of PEM Fuel Cell Systems", *Energy Conversion and Management*, Vol. 160, pp. 486-494, 2018.

[7] S. Ahmadi, S. Abdi, and M. Kakavand, "Maximum Power Point Tracking of a Proton Exchange Membrane Fuel Cell System Using PSO-PID Controller", *International Journal of Hydrogen Energy*, Vol. 42, No. 32, pp. 20430-20443, 2017.

[8] H. Hamedi, R. Khezri, S. Golshannavaz, and B. Ershadifard, "Efficient Voltage Control in Proton Exchange Membrane Fuel Cell: an Approach based on Intelligent Algorithms", *IETE Journal of Research*, Vol. 63, No.2, pp. 216-224, 2017.

[9] N. Chatrattanawet, T. Hakhen, S. Kheawhom, and A. Arpornwichanop, "Control Structure Design and Robust Model Predictive Control for Controlling a Proton Exchange Membrane Fuel Cell", *Journal of Cleaner Production*, Vol. 148, pp. 934-947, 2017.

[10] X. Chen, Y. Fang, Q. Liu, L. He, Y. Zhao, T. Huang, and X. Wang, "Temperature and Voltage Dynamic Control of PEMFC Stack using MPC Method", *Energy Reports*, Vol. 8, pp. 798-808, 2022.

[11] R. Vinu and P. Varghese, "Robust Optimized Artificial Neural Network based PEM Fuel Cell Voltage Tracking", *In Innovations in Bio-Inspired Computing and Applications, Springer, Cham*, Vol. 424, No. 9, pp. 79-91, 2016.

[12] K. J. Reddy and N. Sudhakar, "High Voltage Gain Interleaved Boost Converter with Neural Network based MPPT Controller for Fuel Cell based Electric Vehicle Applications", *IEEE Access*, Vol. 6, pp. 3899-3908, 2018.

[13] M. M. Savrun and M. İnci, "Adaptive Neuro-Fuzzy Inference System Combined with Genetic Algorithm to Improve Power Extraction Capability in Fuel Cell Applications", *Journal of Cleaner Production*, Vol. 299, No. 126944, 2021.

[14] J. Li and T. Yu, "Distributed Deep Reinforcement Learning for Optimal Voltage Control of PEMFC", *IET Renewable Power Generation*, Vol. 15, No. 12, pp. 2778-2798, 2021.

[15] K. E. Dagher, "Design of an Adaptive Neural Voltage-Tracking Controller for Nonlinear Proton Exchange Membrane Fuel Cell System based on Optimization Algorithms", *Journal of Engineering and Applied Sciences*, Vol. 13, No. 15, pp. 6188-6198, 2018.

[16] M. Derbeli, O. Barambones, M. Farhat, and L. Sbita, "Efficiency Boosting for Proton Exchange Membrane Fuel Cell Power System Using New MPPT Method", In: *Proc. of the 10th International Renewable Energy Congress (IREC)*, Sousse, Tunisia, pp. 26-28, 2019.

[17] M. Y. Silaa, M. Derbeli, O. Barambones, and A. Cheknane, "Design and Implementation of High Order Sliding Mode Control for PEMFC Power System", *Energies*, Vol. 13, No. 17, 2020.

[18] S. R. Fahim, H. M. Hasanien, R. A. Turky, A. Alkuhayli, A. A. A. Shamma'a, A. M. Noman, and F. Jurado, "Parameter Identification of Proton Exchange Membrane Fuel Cell based on Hunger Games Search Algorithm", *Energies*, Vol. 14, No. 16, 2021.

[19] J. M. Corrêa, F. A. Farret, J. R. Gomes, and M. G. Simões, "Simulation of Fuel-Cell Stacks Using a Computer-Controlled Power Rectifier with the Purposes of Actual High-Power Injection Applications", *IEEE Transactions on Industry Applications*, Vol. 39, No. 4, pp. 1136-1142, 2003.

[20] A. S. A. Araji, H. A. Dhahad, and E. A. Jaber, "A Neural Networks based Predictive Voltage-Tracking Controller Design for Proton Exchange Membrane Fuel Cell Model", *Journal of Engineering*, Vol. 25, No. 12, pp. 26-48, 2019.

[21] H. A. Dhahad, K. E. Dagher, and A. S. A. Araji, "Design of optimum SIMO-PID neural voltage-tracking controller for non-linear fuel cell system based on comparative study of various intelligent swarm optimization algorithms", In: *Proc. of International Conf. on Sustainable Engineering and Technology (INTCSET 2020)*, Baghdad, Iraq, pp. 1-16, 2020.

[22] H. Qteat and M. Awad, "Using Hybrid Model of Particle Swarm Optimization and Multi-Layer Perceptron Neural Networks for Classification of Diabetes", *International Journal of Intelligent Engineering and Systems*, Vol. 14, No. 3, pp. 11-22, 2021, doi: 10.22266/ijies2021.0630.02.

[23] M. Sinnoor and S. K. Janardhan, "An ECG Denoising Method Based on Hybrid MLTP-EEMD Model", *International Journal of Intelligent Engineering and Systems*, Vol. 15, No. 1, pp. 575-583, 2022, doi: 10.22266/ijies2022.0228.52.

[24] F. N. Moghanloo, A. Yazdizadeh, and A. P. J. Fomani, "A New Modified Elman Neural Network with Stable Learning Algorithms for Identification of Nonlinear Systems", In: *Proc. of Computer and Information Science*, Springer, Cham, pp.171-193, 2015.

[25] A. S. A. Araji, M. F. Abbod, and H. S. A. Raweshidy, "Design of a Neural Predictive Controller for Nonholonomic Mobile Robot based on Posture Identifier", In: *Proc. of the Lasted International Conference Intelligent Systems and Control*, Cambridge, United Kingdom, pp. 198-207, 2011.

[26] G. Ren, Y. Cao, S. Wen, T. Huang, and Z. Zeng, "A modified Elman Neural Network with New Learning Rate Scheme", *Neurocomputing*, Vol. 286, pp. 11-18, 2018.

[27] Z. E. Kanoon, A. S. A. Araji, and M. N. Abdullah, "An Intelligent Path Planning Algorithm and Control Strategy Design for Multi-Mobile Robots based on a Modified Elman Recurrent Neural Network", *International Journal of Intelligent Engineering and Systems*, Vol. 15, No. 5, pp. 400-415, 2022, doi: 10.22266/ijies2022.1031.35.

[28] C. Ziogou, S. Voutetakis, M. C. Georgiadis, and S. Papadopoulou, "Model Predictive Control (MPC) Strategies for PEM Fuel Cell Systems–A Comparative Experimental Demonstration", *Chemical Engineering Research and Design*, Vol. 131, pp. 656-670, 2018.